



HAL
open science

Using Deep Learning to Hedge Rainbow Options

Thibault Collin

► **To cite this version:**

Thibault Collin. Using Deep Learning to Hedge Rainbow Options. Université Paris Dauphine - PSL. 2023. hal-04060013

HAL Id: hal-04060013

<https://hal.science/hal-04060013>

Submitted on 4 Jun 2023

HAL is a multi-disciplinary open access archive for the deposit and dissemination of scientific research documents, whether they are published or not. The documents may come from teaching and research institutions in France or abroad, or from public or private research centers.

L'archive ouverte pluridisciplinaire **HAL**, est destinée au dépôt et à la diffusion de documents scientifiques de niveau recherche, publiés ou non, émanant des établissements d'enseignement et de recherche français ou étrangers, des laboratoires publics ou privés.

Copyright

Using Deep Learning to Hedge Rainbow Options

Thibault Collin ¹

June 6, 2023

Abstract

The general scope of this thesis ² will be to further study the application of artificial neural networks in the context of hedging rainbow options. Due to their inherently complex features, such as the correlated paths that the prices of their underlying assets take or their absence from traded markets, finding an optimal hedging strategy for rainbow options is difficult, and traders usually have to resort to models and methods they know are inaccurate. An alternative approach involving deep learning however recently surfaced in the context of hedging vanilla options [6], and researchers have started to see potential in the use of neural networks for options endowed with exotic features in [5], [12] and [22].

The key to a near-perfect hedge for contingent claims might be hidden behind the training of neural network algorithms [6], and the scope of this research will be to further investigate how those innovative hedging techniques can be extended to rainbow options [22], using recent research [21], and to compare our results with those proposed by the current models and techniques used by traders, such as running *Monte-Carlo* path simulations. In order to accomplish that, we will try to develop an algorithm capable of designing an innovative and optimal hedging strategy for rainbow options using some intuition developed to hedge vanilla options [21] and price exotics [5]. But although it was shown from past literature to be potentially efficient and cost-effective, the opaque nature of an artificial neural network will make it difficult for the deep learning algorithm to be fully trusted and used as a sole method for hedging purposes, but rather as an additional technique associated with other more reliable models.

1 Introduction

The most crucial step in dealing with any asset is to be capable of determining its price, usually referred to in the literature as the *present value*. That price must reflect the reality as closely as possible, because for widely-traded instruments such as options, even the smallest price discrepancy can have severe consequences on the profits and losses made by traders. European options are often

¹Paris Dauphine University student, enrolled in the Master 203 - Financial Markets

²Master thesis written under the direction of Prof. Thibaud Vienne and Prof. Gaelle Le Fol

evaluated using the *Black-Scholes* pricing model [3], which calculates the price of an option as the discounted expected value of its payoffs, under a risk neutral probability measure. The model is arbitrage-free, meaning that no certain gain can be made without taking any risk. Under *Black-Scholes*, the price of an option is dependent on several input parameters, such as the option's time to maturity or the volatility of its underlying's spot price. The evolution of those parameters thus has an influence on the *present value* of the evaluated contingent claim, and each option reacts differently to a variation of one of its inputs. These reactions are characterized by coefficients that are commonly referred to as the *Greeks*, and as it is often preferable for the value of a portfolio to be stable over time, traders usually build theirs so that the *Greeks* are neutralized. This process is referred to as *hedging*. Hedging is thus buying or selling additional instruments to make a portfolio neutral to one or several input variations, because the *Greeks* of the additional assets cancel out with those of our initial portfolio.

Because those sensitivities change constantly during an option's life, traders need to monitor and rebalance their portfolio to maintain their hedge accordingly, but the presence of trading costs prevents the possibility for the hedge to be realized continuously, so it is done periodically. Figuring out exactly the price and *Greeks* of an option at any moment is therefore of paramount importance in that context, because any miscalculation could result in a sub-optimal hedging strategy. This comes down to choosing the most convenient model to begin with, as each model is endowed with a specific set of assumptions that will influence the degree to which the solution is or is not well approximated. For certain types of derivatives such as vanilla options, the present value can be calculated analytically as a closed-form solution. Pricing options with more exotic features rarely allows for such, and numerical approximations using *Monte-Carlo* [4] simulations are often required. Those methods have however proven to be computationally expensive and tremendously slow to run when there is some complexity involved, and in a context where the parameters of an option are updated regularly, *Monte-Carlo* appears to be rather unreliable.

Our study will have a particular focus on rainbow options, which are exotic derivatives relying on the performance of more than a single underlying asset. These instruments are of interest not only because of their popularity, but also because their dependence over multiple underlying assets with correlated paths makes it difficult to define an optimal hedging strategy that is in line with real-world dynamics, especially since current methods cannot account for very sudden and extreme market moves, forcing traders to use their experience and intuition to manually re-calibrate their strategy, which has gotten increasingly difficult with the growing sophistication of financial markets. This explains why traders have been looking for an innovative method that would assist them in reaching an optimal hedging strategy for rainbow options, and improvements could be foreseen through the use of deep learning and artificial neural networks [6], an architecture capable of learning key representations in the data without the need for an underlying model. The application of neural networks to hedging and pricing purposes was proven successful in several research papers, and was initiated by [17], who demonstrated an ability of deep learning in pricing futures options.

The studies of [9] then illustrated how neural networks could outperform standard hedging models for American options, and [6] presented an extensive theoretical framework for hedging vanilla options in the presence of market frictions, which was later applied by [21], who analyzed the calibration of the algorithm to various stochastic paths for the asset prices, with interesting results. Studies diving further into the use of deep learning for exotic derivatives include [22], who used the *regress later neural network* technique to price and semi-statically hedge high-dimensional contingent claims such as *Bermudan max* and *basket options*, which came after the works of [5], whose paper initiated research for options relying on several underlyings, namely *rainbow options*. Those were further explored by [12], who illustrated the feasibility of the deep learning approach through the valuation of an option relying on six underlying assets, as well as its computational power when

compared to *Monte-Carlo* simulations, showing improvements in speed and accuracy.

This paper will partly aim at extending the most recent literature made on using deep learning for dealing with problems of hedging vanillas and pricing exotics, to the problem of hedging rainbow options in a regular market context. Beyond designing a strategy that would be in line with real-world dynamics, using deep learning could also allow us to eliminate constraints that weight heavily in the accuracy of our results, such as the absence of sudden and extreme market moves. We will therefore try to implement the algorithm in a context that is closer to what is really observed on the markets, to investigate the potential of deep learning in areas that could not have been explored by current methods, due to the high degree of complexity and computational power that was required.

The thesis shall be structured as follows. We will successively cover prerequisites in financial mathematics (*Chapter 2*) as well as in general deep learning concepts (*Chapter 3*), to lay down the basic foundations of our research. Then, as we begin building and testing our neural network algorithm, we will first produce and interpret the hedging strategy designed by the algorithm for European Call options, using *Black-Scholes* as a benchmark (*Chapter 4*). Having shown the robustness and efficiency of the method for vanilla options, we will then derive an adjustment of the algorithm for rainbow options (*Chapter 5*), in which we shall also test the accuracy of the method in the presence of large and unexpected market moves, to assess whether the neural networks are able to properly process such information to adapt the hedging parameters accordingly. To conclude, we shall condense our results and infer on the practical feasibility and usefulness of the method, and we shall also further discuss issues and limits encountered with deep learning algorithms applied in such context, as well as providing potential clues for further developments (*Chapter 6*).

2 Mathematical prerequisites

2.1 Agent's terminal wealth

We will need to consider a discrete-time financial market with trading dates comprised in the set $\{0, t_1, t_2, \dots, t_n\}$ with $t_n = T$ our finite time horizon, as well as a complete probability space $(\Omega, \mathcal{F}, \mathbb{P})$ with $\Omega = \{\omega_1, \dots, \omega_n\}$ and \mathbb{P} the risk-neutral probability measure, which is not the observed measure, but an identical one that is fitted for arbitrage-free pricing. Let us also define the set of all random variables over Ω to be \mathbb{Q} , such that $\mathbb{Q} := \{Q : \Omega \rightarrow \mathbb{R}\}$.

Let us denote I_i any new piece of information that becomes available at time t_i . This may include mid-prices of liquid instruments, trading signals and more. All information available up to a certain time t_i is thus given by the filtration $\mathbb{F} = (\mathcal{F}_i)$ for $i = 0 \dots n$, which is generated by the process $I = (I_i)$ for $i = 0 \dots n$. In this study, we will restrain the information set to the *log-transformed* prices of the assets considered. The prospect of implementing sophisticated trading signals will be explored in *Chapter 6* as a further research.

We will then assume that m instruments exist in the market for us to hedge our contingent claim, and that their mid-prices follow an \mathcal{F} -adapted process $\mathbb{S} = (S_i)$ for $i = 0 \dots n$. Those additional instruments can either be equities or European options, and their maximum maturity is T . The portfolio of contingent claims we intend to hedge will be denoted Z . The position we will take in the hedging instrument t is given by the \mathcal{F} -adapted stochastic process $\delta = (\delta_i^t)$ for $i = 0 \dots n$ and $t = 1 \dots m$. Finally, we define the set of all such trading strategies to be \mathcal{H} .

We note the profits made from trading the hedging instrument at time i to be $(\delta \cdot S)_i$, which gives the following total gains and losses until maturity.

$$(\delta \cdot S) = \sum_{i=0}^{n-1} \delta_i \cdot (S_{i+1} - S_i)$$

Trading is costly through many ways: bid-ask spreads or liquidity constraints for example. Let us define by c_i the cost of taking a position at time t_i on any asset. The total cost of trading is then defined as the following.

$$C(\delta) = \sum_{i=0}^n c_i \cdot (\delta_i - \delta_{i-1})$$

To simplify, let us assume that no position is held in hedging instruments outside $\{t_1, t_2, \dots, t_{n-1}\}$. Finally, the self-financing strategy starts with an initial lump sum p_0 . The agent's terminal wealth is then defined as the following [6].

$$P_n L(Z, \delta, p_0) = p_0 - Z + (\delta \cdot S) - C(\delta) \quad (2.1)$$

The goal is to minimize said equation, being the part of our position that we were not able to hedge. In other terms, it is our final *risk exposure*. We shall see that the objective of the algorithm will be to find a *hedging strategy* δ such that the uncovered risk is minimal. Note that this equation can be extended to a *hedging strategy* on two underlyings. Indeed, in *Chapter 5* we shall study options relying on two underlying assets, and we would want to hedge against both their moves.

$$P_n L(Z, \delta_1, \delta_2, p_0) = p_0 - Z + (\delta_1 \cdot S_1) - C(\delta_1) + (\delta_2 \cdot S_2) - C(\delta_2) \quad (2.2)$$

Let us finally remark that we would be able to perform such strategy with or without trading costs, although they were usually implemented for *vanilla option* hedging in the past literature with [6], [7] and [21].

2.2 Convex risk measures

We introduce *monetary risk measures* denoted ρ , which are statistical measures used to assess the risk inherent to an investment, taking the form of a cash requirement. We then have that for any portfolio of assets X , $\rho(X)$ can be viewed as the minimal amount of cash required for the risk of the position to be in an acceptable range, in light of the agent's preferences. We will therefore materialize the aforementioned *unhedged* part of our position by said risk measure, which our algorithm will try to minimize. To guarantee that the solution we find is close-to-optimal, we choose to work with *convex risk measures*, which are classic risk measures satisfying the following properties. Once again, this minimization program can be extended to a strategy involving two underlying assets.

Definition 2.1 *We let X_1 and $X_2 \in \mathcal{X}$ be positions in assets. We let $\rho : \mathcal{X} \rightarrow \mathbb{R}$ be a convex risk measure if the following properties are verified.*

- $X_1 \geq X_2 \rightarrow \rho(X_1) \leq \rho(X_2)$ (*monotone decreasing*)
- $\rho(\beta X_1 + (1 - \beta)X_2) \leq \beta \rho(X_1) + (1 - \beta)\rho(X_2)$ (*convex*)
- $\rho(X_1 + c) = \rho(X) - c, \quad \forall c$ (*translation invariance*)

Having introduced a proper way of quantifying the risk of our portfolio then allows us to introduce the agent's optimization program. Let us denote by $\pi(X)$ the minimal lump sum required by the agent's preferences for the position in a portfolio of financial assets X to be sufficiently well hedged, \mathcal{H} the set of possible trading strategies, and $\delta \in \mathcal{H}$ the minimizing strategy for the program [6].

$$\pi(X) = \left(\inf_{\delta \in \mathcal{H}} \rho(X + (\delta \cdot S) - C(\delta)) \right) \quad (2.3)$$

We thus have that the minimal cash injection π that is required to make a portfolio X acceptable regarding an agent's preferences is equal to the minimal lump sum required to make the *hedged-portfolio* acceptable in light of those same preferences, with $\delta \in \mathcal{H}$ the hedging strategy allowing such. In (2.2), π is monotone decreasing and translation invariant. Given that the function C and the set \mathcal{H} are convex, π then is a convex risk measure [6].

Finally, as we need to consider the scenario in which having no liabilities may generate positive expected returns, which could happen under the physical measure, we decide to focus on the *indifference price* denoted $p(Z)$. This price is such that holding $p(Z)$ and a position $-Z$ gives the same utility as holding nothing.

$$\pi(p(Z) - Z) = \pi(0) \rightarrow p(Z) = \pi(-Z) - \pi(0) \quad (2.4)$$

This result is given by translation invariance, as π is a convex risk measure.

2.3 Optimized certainty equivalents

In this study, we want to use a specific class of convex risk measures denoted *optimized certainty equivalents* (or *OCEs*), to determine the minimal amount of cash required to make a portfolio of contingent claims acceptable in light of some agent's preferences. We denote X such a portfolio and $r \in \mathbb{R}$ the minimizing parameter of our program.

Definition 2.2 We let $l: \mathbb{R} \rightarrow \mathbb{R}$ be a convex risk measure and denote it our loss function. The OCE is then defined as the following.

$$\rho(X) = \inf_{r \in \mathbb{R}} \{r + \mathbb{E}[l(-X - r)]\}, X \in \mathcal{X} \quad (2.5)$$

Following the intuition built in [6], the *entropic risk measure* can be used in our algorithm. and it can be defined with the following formula.

Definition 2.3 For a fixed and positive λ we set $l(x) = e^{\lambda x} - \frac{1 + \ln(x)}{\lambda}$. Optimizing and using (2.4) gives us the entropic risk measure.

$$\rho(X) = \frac{1}{\lambda} \ln(\mathbb{E}[e^{-\lambda X}]) \quad (2.6)$$

Such risk measure has for long been quite popular in financial mathematics because of some interesting properties it is endowed with, as it depends on an agent's risk aversion, and can be modelled through exponential utility functions, which are defined as $U(x) = -e^{-\lambda x}$ with λ the positive *risk aversion coefficient*. We notice how the aforementioned utility function appears in the entropic risk measure (2.7), but let us solidify the relationship between the two with the following proposition [6].

Proposition 2.4 *Let $q(Z)$ be a solution of the following indifference pricing problem. Then it follows that $q(Z) = p(Z)$, the latter being the indifference price.*

$$\sup_{\delta \in \mathcal{H}} \mathbb{E}[q(Z) - Z + (\delta \cdot S) - C(\delta)] = \sup_{\delta \in \mathcal{H}} \mathbb{E}[U\{(\delta \cdot S) - C(\delta)\}]$$

This result means that if we receive $q(Z)$ of cash in exchange for letting Z go, we are not better nor worse off compared to not selling Z at all.

2.4 Reminders on probability distributions

Several probability distributions are to be used along this paper to model the uncertain character of our dynamics. Their density function and relevance for our study are to be successively and concisely introduced in this section.

Gaussian distribution

The univariate normal distribution is by far the most popular of all probability distributions, and will be used here mainly in the discretization of a *Brownian* motion inherent to the price dynamics of a single asset, as well as the computation of the prices and *Greeks* for our options (*Chapter 4*).

Definition 2.5 *We denote $f(x)$ the probability density function of a Gaussian distribution, with μ and σ its expectation and standard deviation. If $X \sim \mathcal{N}(\mu, \sigma)$ then X is a Gaussian, and if $X \sim \mathcal{N}(0, 1)$ then X is a standard Gaussian variable.*

$$f(x) = \frac{1}{\sigma\sqrt{2\pi}} e^{-\frac{1}{2}\left(\frac{x-\mu}{\sigma}\right)^2}$$

Multivariate Gaussian distribution

Such is an extension of the univariate case to account for the joint moves of two underlying assets, and is to be used for the same purpose as the preceding distribution, but for multi-asset price dynamics (*Chapter 5*).

Definition 2.6 *Given a symmetric positive definite covariance matrix \mathcal{M} and μ the expectation of the distribution, we denote $f_X(x_1, \dots, x_k)$ the multivariate normal density per the following, with X being a k -dimensional column vector.*

$$f_X(x_1, \dots, x_k) = \frac{\exp\{-\frac{1}{2}(x - \mu)^t \mathcal{M}^{-1}(x - \mu)\}}{\sqrt{(2\pi)^k |\mathcal{M}|}}$$

We will mainly be interested in the cumulative distribution of such variable, for which there does not exist any closed-form solution. Therefore, the computation will be made following the efficient algorithm introduced in [11].

Poisson distribution

The discrete Poisson distribution can describe the probability of occurrence for some rare events, and is to be used to model for the presence of jumps in the multi-asset dynamics, for which random samples are to be generated from a *Poisson* distribution (*Chapter 5*).

Definition 2.7 For a given parameter λ and x the number of events occurring within λ , we define as f the probability mass function of a Poisson distribution.

$$f(x, \lambda) = \frac{\lambda^k e^{-\lambda}}{k!}$$

Exponential distribution

To simplify our computations, we decided to use a proxy for the *Laplace* distribution to measure the size of our jumps. Such proxy, that is to be defined later, involves a multivariate *Gaussian* as well as an *exponential* distribution.

Definition 2.8 For a given parameter $\lambda > 0$, we define as f the probability density function of an exponential distribution over any $x \geq 0$.

$$f(x, \lambda) = \lambda e^{-\lambda x}$$

2.5 Additional risk measures

The *entropy* is not the only common risk measure used in the literature. We will work with the *mean squared error* to hedge multi-asset options in *Chapter 5*, as it was shown to provide stronger results when compared to other risk measures. In the context that will be ours, we will minimize the *wealth* function, meaning that the predicted value is ideally 0. Finally, we will use $n = 1.2 \cdot 10^5$ because our entire data set will be comprised of as many data points.

Definition 2.9 For n the number of data points, Y_i the observed values and \hat{Y}_i the predicted values, we define the mean squared error as the following risk function.

$$mse = \frac{1}{n} \sum_{i=1}^n (Y_i - \hat{Y}_i)^2 \tag{2.7}$$

3 Neural Networks

3.1 Understanding key notions

Deep learning architecture

Deep learning algorithms are structures endowed with the ability to learn features and patterns directly from data they are trained on, in order to figure out similar patterns on resembling new data they have never seen. Through successive layers of neurons which are connected by channels to form the *neural network*, data is analyzed by the algorithm and patterns are understood.

The *training set* is defined as the set of inputs and their respective expected outputs which are initially fed to the algorithm. Through this first set, the algorithm will try and figure out what are the most fundamental and important representations behind the data. The *testing set* is then given as a way of assessing whether the neural network managed to seize and project those patterns on new but similar data. Measuring its performance is thus done through the *loss function*, which compares the actual outcome of the algorithm with what we expect to obtain. The loss function that shall be used is the *entropic risk measure* defined in (2.6), unless stated otherwise.

Learning is done iteratively until the loss function is minimized. Inputs are initially fed into the network through first layers of neurons, called the *input layers*. They are then transferred to subsequent *hidden layers*, whose role is to decipher key representations of the data. Each neuron in those layers has its own importance in the algorithm, meaning that the weights attached to the inputs of each neuron, as well as their bias, is different. These parameters are randomly initialized and iteratively adjusted through *back-propagation*, which is what allows neural networks to learn by themselves, by evaluating their performance using the loss function. The *weights* are allocated to each input entering a given neuron, and the *bias* term skews the result of the neuron's output, modelling a systemic error stemming from incorrect assumptions on the model. To resume, the algorithm will iteratively rearrange its structure until the output is judged sufficiently close to what the network is expected to produce.

We just introduced the feed-forward neural network, a structure where neurons only communicate horizontally. Such will form the basic element in our research and is defined in the following definition.

Definition 3.1 Let $L, N_0, \dots, N_L \in \mathbb{R}, \sigma_i : \mathbb{R} \rightarrow \mathbb{R}$ and let A_i be affine functions, for any $i \in \{1, 2, \dots, L\}$. The function $\mathcal{F} : \mathbb{R}^{N_0} \rightarrow \mathbb{R}^{N_L}$ below is called a feed-forward neural network, with $\mathcal{F}_i = \sigma_i \circ A_i$ for any $i \in \{1, 2, \dots, L - 1\}$.

$$\mathcal{F}(x) = A_L \circ \mathcal{F}_{L-1} \circ \dots \circ \mathcal{F}_1 \tag{3.1}$$

Activation functions

We define σ_k as the *activation function* applied to the neuron k . Such function decides on the degree of activation of the node, depending on the accuracy and relevance of its output. Denoting b the bias and w the weights associated with the inputs x gives us the following final output o_k for a given neuron k .

$$o_k = \sigma \left(\sum_{i=1}^n (w_i x_i) + b_k \right)$$

The choice for an activation function is crucial, and is made by evaluating the trade-off between simplicity of implementation and powerfulness. Indeed, complex activation functions allow nodes to learn complex structures in the data. Nonlinear functions are examples of such functions, whereas linear ones are easier to implement and faster to run. Both accumulate their share of advantages and shortcomings, so our idea will be to use one that is a mix of both.

Let us work with an activation function that resembles a linear function, while in reality being a nonlinear one, allowing for complex relationships in the data to be learned while allowing fast computations. Such is called the *rectified linear activation unit (ReLU)* [10]. That function is often referred to as *piecewise linear*, for it is half linear and half nonlinear. It is defined as the positive part of its input: $\sigma(x) = \max(0, x)$. One can therefore see that the gradient is zero when x is negative, and the neuron becomes inactive.

Recurrent neural networks

We note L the total number of layers and N_i the dimension of the layer i . Finally, let us consider $L - 1$ hidden layers, one input and one output layer. We would want our algorithm to remember to some extent what happened in the past, because we need to consider market frictions. In that sense, we could extend our regular feed-forward neural network so that a temporal dynamic behavior can appear. This would be done through the use of *recurrent neural networks (RNNs)*, where neurons use their memory regarding past information in their decision-making process. Such an algorithm is structured as an ensemble of regular feed-forward neural networks where information is passed both horizontally to the next hidden layer, and vertically to a similar hidden layer at the next time period. For the rest of this paper, we shall however restrain ourselves to *simple* neural networks, and leave *recurrent* ones for further exploration. To conclude, we shall explain the mechanism that allows the algorithm to adjust its weights and biases, to converge towards their final values.

Stochastic gradient descent algorithms

In our model, we will use the *Adam* algorithm [18], which is defined as a *stochastic gradient descent algorithm* with advantageous properties. As was explained earlier in that sub-section, the neural network algorithm works under a loss function that is aimed to be globally minimized, explaining why the function needed to be differentiable. A stochastic gradient descent algorithm loops through the network and uses at each iteration the set of first partial derivatives ∇ of the loss function $l(\theta)$ that was calculated using *back-propagation*, and iteratively takes a step downhill using the gradient. This means that the next point $\theta^{(i+1)}$ taken shall always be lower than the previous one $\theta^{(i)}$, in order to reach a global minimum for the loss function. The starting point is often randomly initialized.

$$\theta^{(i+1)} = \theta^{(i)} - \eta \nabla_i \left(\theta^{(i)} \right)$$

The key idea behind such a process is to quantify the step taken by the algorithm to move downhill the loss function. That step η is called the *learning rate*, and it is a small fixed hyper-parameter for regular gradient descent algorithms. For the *Adam algorithm* however, the learning rate of each input parameter is being individually and adaptively optimized, and under suitable assumptions on the loss function l as well as on the sequence $\{\eta_i\}$ for $i \in \mathbb{N}$, $\theta^{(i)}$ converges to a local minimum of l as $i \rightarrow \infty$, with dynamics for updating parameters resembling what we already saw above, but using instead the first two moments of the gradient ∇ respectively denoted m and v , with α and β being *forgetting factors*, and ϵ a small scalar preventing any division by zero.

$$m_{\theta}^* = \left(\frac{1}{1 - \alpha} \right) \left(\alpha m_{\theta}^{(i)} + (1 - \alpha) \nabla l_i(\theta^{(i)}) \right)$$

$$v_{\theta}^* = \left(\frac{1}{1 - \beta} \right) \left(\beta m_{\theta}^{(i)} + (1 - \beta) (\nabla l_i(\theta^{(i)}))^2 \right)$$

$$\theta^{(i+1)} = \theta^{(i)} - \eta \frac{m_{\theta}^*}{\sqrt{v_{\theta}^* + \epsilon}}$$

Combining the *stochastic gradient descent* algorithm with the *back-propagation* error algorithm makes the process of computing ∇ efficient, and is at the core of the deep learning approach [10].

3.2 Validity and power of the method

Having clearly defined the main concepts attached to the deep learning approach, let us now introduce mathematical proof for both the power and the validity of such method. Let us coin as $\mathcal{NN}_{\infty,e,f}^{\sigma}$ the set of all neural networks mapping from $\mathbb{R}^e \rightarrow \mathbb{R}^f$ with activation function σ . Let us denote as $\mathcal{NN}_{M,e,f}^{\sigma}$ the one with at most M non-zero weights and a potentially infinite number of layers. The following theorem [6] proves the validity of the method, as it shows the algorithm is able to provide us with the minimal cash injection that the agent must supply to hedge his claim given his preferences, while the number of non-zero weights in the neural network tends towards infinity.

Theorem 3.2 *Let \mathcal{H}_M denote the subspace of all strategies δ that can be obtained with the use of neural networks belonging to $\mathcal{NN}_{M,e,f}^{\sigma}$ with X an asset position and ρ and π^M convex risk measures.*

$$\lim_{M \rightarrow +\infty} \pi^M(X) = \lim_{M \rightarrow +\infty} \left(\inf_{\delta \in \mathcal{H}_M} \rho(X + (\delta \cdot S) - C(\delta)) \right) \quad (3.2)$$

An important theorem [16] then illustrates that the feed-forward neural network is able to provide accurate approximations for multivariate functions, demonstrating the usefulness of the method.

Theorem 3.3 (Universal approximation [16]). *Let σ be bounded and non-constant and ρ a finite risk measure. The following statements are true.*

- $\forall \rho$ on $(\mathbb{R}^e, \mathcal{B}(\mathbb{R}^e))$ and $p \in [1, +\infty[$, the set $\mathcal{NN}_{\infty,e,f}^{\sigma}$ is dense in $L^p(\mathbb{R}^e, \rho)$.
- If in addition $\sigma \in C(\mathbb{R})$, then the set $\mathcal{NN}_{\infty,e,f}^{\sigma}$ is dense in $C(\mathbb{R}^e)$ for the topology of uniform convergence on compact sets (or compact convergence).

This last statement explains that having an activation function that is continuously differentiable on \mathbb{R} while having the set of all neural networks to be dense on the Lebesgue space (\mathbb{R}^e, ρ) ensures that the solution given by the neural network algorithm is close-to-optimal.

Properties 3.4 *Having $\{\mathcal{NN}_{M,e,f}^{\sigma}\}_{M \in \mathbb{N}}$ a sequence of subsets from $\{\mathcal{NN}_{\infty,e,f}^{\sigma}\}$, we can give the following properties $\forall M \in \mathbb{N}$.*

- $\{\mathcal{NN}_{M,e,f}^{\sigma}\} \subset \{\mathcal{NN}_{M+1,e,f}^{\sigma}\}$ and $\bigcup_{M \in \mathbb{N}} \mathcal{NN}_{M,e,f}^{\sigma} = \mathcal{NN}_{\infty,e,f}^{\sigma}$.
- $\mathcal{NN}_{M,e,f}^{\sigma} = \{F^{\theta} : \theta \in \Theta_{M,e,f}\}$, $\Theta_{M,e,f} \subset \mathbb{R}^g$ for $g \in \mathbb{N}$ (depending on M).

This sequence could be thought of as the subset of all neural networks with a fixed number of nodes and hidden layers, parametrized by a vector θ whose dimension g depends on M [21]. The following and final part of this chapter will implement all the concepts previously introduced, in the context of hedging derivatives.

3.3 Deep learning in the context of hedging

Let us remember that the aim of our deep learning algorithm is to produce the hedging strategy $\delta \in \mathcal{H}_M$ as a numerical solution for the problem of hedging *vanilla* and *rainbow* options. Theorem 3.1 provided proof of validity for the method, and Theorem 3.2 justified the usefulness and accuracy of the approach.

The feasibility of the algorithm shall then be demonstrated in the following sections by building and training the neural network in Python with the use of *Tensorflow* [10]. Both training and testing sets that are to be used in the development of the algorithm will be composed of underlying asset paths, generated randomly using *Numpy*.

The deep learning approach to hedging any claim will follow the same structure. We begin by generating samples of asset paths endowed with specific price dynamics, which will then be fed to the algorithm. Using the *wealth* function, the network will search for the hedging strategy that minimizes the residual cash injection, materialized by the *entropic risk measure* (2.7). By the end of that *training* period, the algorithm should have learned an approximated relationship between the spot moves and the strategy to adopt, and we can move to the *testing* phase. Here, the algorithm tries to produce the *hedging parameters* according to what was learned in the previous training phase. What is produced is then compared with what the benchmark outputs.

As was introduced previously, the network shall be trained following the *Adam algorithm* [18], with $\eta = 0.005$ as an initial learning rate that is then individually adjusted. As was explained earlier, all the parameters of the network shall be randomly initialized from a range depending on the size of the preceding layer, increasing the pace at which the algorithm is able to determine the minimum of the loss function [14]. For efficiency purposes, we use a *batch size* of 500, which is the number of samples that are processed before the structure of the algorithm is updated. Finally, the *ReLU* activation function [10] is to be applied to our hidden layers, unless stated otherwise. The complete code can be found and used on a *GitHub* page in the repository: *thibaultcoo/rainbow-deep-hedging*.

4 Deep Hedging Vanillas

4.1 Fundamental derivatives pricing theory

Black-Scholes model

The *Black-Scholes* equation for pricing European options [3] is widely seen as one of the most popular pieces of research that was produced in recent financial mathematics, because of its efficiency and usefulness under its restrictive set of assumptions. Indeed, given continuous rebalancing and assuming the complete set of assumptions is verified, the payoffs of an option can be perfectly replicated, hence allowing for a complete hedge over any move of the underlying's spot price.

Definition 4.1 *Given all relevant assumptions are verified, the Black-Scholes price of a European Call option is given by the following equation.*

$$V(t, S_t) = e^{-q(T-t)} S_t \mathcal{N}(d_1) - e^{-r(T-t)} KN(d_2) \quad (4.1)$$

Let \mathcal{N} be the cumulative distribution function of a standard normal random variable, r and q the constant parameters for the interest and dividend rate, σ the underlying's volatility, T the option's maturity, K the strike price and S_t the underlying's price at time t . The input parameters for \mathcal{N} are described below.

$$d_1 = \frac{1}{\sigma\sqrt{T-t}} \left(\ln \left(\frac{S_t}{K} \right) + \left(r + \frac{\sigma^2}{2} \right) (T-t) \right)$$

$$d_2 = d_1 - \sigma\sqrt{T-t}$$

This analytical solution is obtained by solving the *Black-Scholes* parabolic partial differential equation [3], assuming S_t follows a *geometric Brownian motion*.

$$\frac{\partial V}{\partial t} + \frac{1}{2}\sigma^2 S^2 \frac{\partial^2 V}{\partial S^2} + rS \frac{\partial V}{\partial S} - rV = 0 \quad (4.2)$$

From either (4.1) or (4.2) emerges a key hedging parameter, considering we want to hedge the *Call option* against the moves of the underlying's spot price. Such a coefficient is denoted δ , and represents the sensitivity of the option's price to any move of the underlying's price. It is derived from *Black-Scholes* that to perfectly *delta-hedge* the position, one must trade δ unit of the underlying.

$$\delta = \frac{\partial V}{\partial S} = \mathcal{N}(d_1) \quad (4.3)$$

The benchmark will hedge the *Call option* periodically using that parameter. Using *Black-Scholes* however comes at a cost, one of which is the lack of accuracy that the method tends to display, and another being the inability of the model to efficiently evaluate complex options, which we will focus on in *Chapter 5*.

Monte-Carlo method

Using *Monte-Carlo* simulations [4] is a wide-spread solution to deal with those shortcomings. The idea behind *Monte-Carlo* is that a large number of risk-neutral price paths for the underlying asset are generated, following a specific dynamic. For each of those paths, the option's payoff at maturity is computed, and the final value of the option is calculated as the discounted average of those payoffs, which approximates the true price of the option.

The accuracy of the method relies on the *Law of Large Numbers*, which states that the sample average converges almost surely to the expected value. This method allows to fit in any stochastic process for our underlying with potentially interesting features that are more in-line with real-world dynamics, such as the presence of jumps in the underlying's prices. Another benefit is its ability to deal with complexity in options.

We will later study the use of *Monte-Carlo* for options relying on several underlying assets, illustrating the accessibility and popularity of the method for any type of exotics, even though it is computationally heavy and takes an incredible amount of time to run, the problem being the unavailability of more efficient alternatives. So, as an input for our deep learning algorithm in this section, we will run *Monte-Carlo* simulations on an underlying asset for two specific price dynamics separately, *Black-Scholes* and *Heston*. We will then compare the hedging strategies that come along with those dynamics, and compare them with what the benchmark produced for the same underlying.

Under the *Black-Scholes* framework, the dynamics of the underlying asset is governed by the *geometric Brownian motion* defined below [2], with μ and σ being \mathcal{F}_t -adapted processes, and B_t being a Brownian motion.

$$dS_t = \mu S_t dt + \sigma S_t dB_t$$

Definition 4.2 For a given filtration $\mathbb{F} = (\mathcal{F}_i)$ for $i = 0 \dots n$, we define the Brownian motion B_t as a continuous \mathcal{F}_t -adapted process with $B_0 = 0$ and Gaussian stationary and independent increments, such that $B_t - B_s \sim \mathcal{N}(0, t - s)$.

The *discretized Black-Scholes* dynamics will be used as a first set of inputs for our algorithm, assuming that returns are log-normally distributed with unconstrained borrowing and lending at rate r . We finally assume one can buy and sell any amount of the underlying asset in a market without any trading costs. When the price dynamics are evaluated under the risk-neutral measure \mathbb{P} , we have that $\mu = 0$ [2]. We shall use the log transform to generate our paths, with $s_t = \ln(S_t)$.

$$ds_t = -\frac{\sigma^2}{2} dt + \sigma_t dB_t$$

The time discretization of such path then takes the following form under \mathbb{P} , with the time interval $[0, T]$ defined in *Chapter 2*, and using N time steps with $i = 0 \dots n$.

$$s_t = s_{t-1} - \frac{\sigma^2}{2} \frac{T}{N} + \sigma \sqrt{\frac{T}{N}} Z_i \quad (4.4)$$

In the above, Z_i are independently distributed standard normal random variables.

Heston model

To allow for a more compelling analysis of the efficiency of our deep learning architecture, let us introduce another model for which the volatility of the underlying is considered as a stochastic process, in order to get us closer to real market dynamics. We choose to work with the *Heston* model [15], under which the underlying's dynamics S_t are defined below.

$$dS_t = rS_t dt + \sqrt{v_t} S_t dB_t^s, \quad S_0 \geq 0$$

Heston is a *stochastic volatility* model, so we must also define the *Cox-Ingersoll-Ross* dynamics followed by the underlying's volatility v_t , with ξ its own volatility, θ its mean and κ its mean-reversion rate.

$$dv_t = \kappa(\theta - v_t)dt + \xi \sqrt{v_t} dB_t^v, \quad v_0 \geq 0$$

Let us denote B_t^s and B_t^v two Brownian motions, whose correlation will be defined as ρ , where r denotes the risk-free rate, κ is the mean-reversion pace of the process, ξ is the volatility of the volatility and θ is the long-term variance.

Properties 4.3 The volatility process v_t is defined as strictly positive if the following condition, known as the *Feller condition*, is respected.

$$2\kappa\theta \geq \xi^2$$

As for *Black-Scholes*, let us use the *discretized* log-transformed paths for *Heston*, so that it can be applied to the context of periodical hedging. We are still using the time interval $[0, T]$, with N time steps and $s_t = \ln(S_t)$ for $i = 0..n$.

$$s_t = s_{t-1} + r - \frac{v_{t-1}}{2} \frac{T}{N} + \sqrt{v_{t-1}} \sqrt{\frac{T}{N}} Z_i^S \quad (4.5)$$

We perform the same transform with the dynamics of the volatility. We previously used $Z_i^S \sim \mathcal{N}(0, 1)$, and to account for the relationship between the spot and volatility's dynamics, we introduce the following formula to characterize the jiggling of the volatility: $Z_i^V = \rho Z_i^S + \sqrt{1 - \rho^2} Z_i$, where Z_i^V and $Z_i \sim \mathcal{N}(0, 1)$. Let the following be the dynamics of the volatility, with $\varrho_t = \ln(v_t)$ for $i = 0..n$.

$$\varrho_t = \varrho_{t-1} + \frac{1}{v_{t-1}} \left(\kappa(\theta - v_{t-1}) - \frac{\xi^2}{2} \right) \frac{T}{N} + \left(\frac{\xi}{\sqrt{v_{t-1}}} \right) \sqrt{\frac{T}{N}} Z_i^V \quad (4.6)$$

Those paths will be generated in Python using *Numpy*, for both our *training* and *testing* sets. Those random paths will be used to evaluate the robustness of our artificial neural network, which shall then be compared to the hedging parameters generated using *Black-Scholes*'s partial differential equation.

To resume, we will on one hand generate stochastic price paths for the underlying, feed them to the neural network algorithm so that it can decipher key patterns in that data, and produce hedging parameters accordingly. On the other hand, we will compute the *Black-Scholes* hedging parameters, which will allow us to compare and thus evaluate the performance of the deep learning architecture. Such reasoning shall also be observed for when we will study *multi-asset options*, the sole difference being the growing complexity in the methods used.

Calibration of Heston parameters

Several constant parameters need to be introduced to model the dynamics defined above. The process of searching for parameters that are best-suited to fit with real market dynamics is the model *calibration* problem. Such is solved by comparing the analytical price of vanilla options to their market value, and iteratively adjusting the parameters so as to minimize the difference between the two.

A formula for the analytical price of a European call option considering *Heston* dynamics and defined as a function of those parameters was introduced by [8], which the authors later used to calibrate the *Heston* model based on a real data set of 144 vanilla call options with varying maturities from the year 2003. Their results shall be used in this study and will be introduced later.

The pricing formula defined by [8] is the following, with K the strike price and T the time to maturity. One can notice that this analytical solution takes the form of a Fourier transform [24]. This will allow for the computation of the complete option surface using *fast Fourier transform*, an algorithm capable of calculating the *discrete Fourier transform* of a sequence in an efficient manner.

$$C(K, T) = \left(\frac{e^{-0.75 \ln(K)}}{\pi} \right) \int_0^{+\infty} e^{-i v \ln(K)} \eta(v) dv$$

$$\eta(v) = \frac{e^{-rT} \phi(v - (\alpha + 1)i, T)}{\alpha^2 + \alpha - v^2 + i(2\alpha + 1)v}$$

From that equation, we denote ϕ the characteristic function of the log-spot dynamics of the underlying asset, defined as such by [15] in its most simple form.

$$\phi(u, t) = E \left(e^{iu \ln(S_t)} | S_0, \sigma_0^2 \right) \quad (4.7)$$

The detailed equation can be found in [15]. The *fast Fourier transform*-based methods are very popular when it comes to pricing vanilla options, for they allow the simultaneous computation of option values for a ladder of different strike levels. The complexity of (4.7) can make the computations time-consuming, and being able to make simultaneous calculations saves time, which is why they were used in [24] for such calibration.

4.2 An extensive literature review

Several interesting papers have emerged since [17] demonstrated an ability of artificial neural networks to price futures options with great accuracy. The works of [9] extended such studies to *delta* and *vega* hedging problems for vanilla options, whose novelty was to introduce a training set of *price changes* instead of *simple prices*, which resulted in more accurate hedging ratios, as the sensitivities produced by the algorithm were better than when using the standard model.

The most important piece of research in the field of *deep hedging vanillas* is widely seen as being [6], where the authors laid down extensive mathematical foundations to the use of deep learning towards vanilla options hedging. By using *convex risk measures* as loss functions for the algorithm in a context with trading costs, the paper demonstrates that given the trajectories of all hedging instruments, with payoff samples and associated weights, deep learning techniques can be used to compute close-to-optimal hedging parameters, for any transaction cost structure and risk measure. The algorithm was tested under regular *Brownian* dynamics, as well as with *Heston* dynamics, the latter allowing for trading in both the stock and a *variance swap* to complete the market. Beyond using the theoretical notions defined in the paper, we have also been influenced by the general architecture of their algorithm for our own research, although under *Heston* we chose not to introduce the *variance swap* for simplicity.

The need to verify the robustness of the method was then further explored by [21], whose intuition was to test the algorithm under different stochastic dynamics, with some introducing *jump diffusion* in the price of the assets, with *Bates* and *Variance-Gamma* dynamics, although the resulting parameters under the latter were far from being satisfying. An interesting loss function defined as a mix of two expected shortfalls was however introduced, with promising results.

The paper of [7] finally demonstrated that fully *delta-hedging* is sub-optimal, and that depending on how the current holding of underlying assets compares to the quantity recommended by said *delta-hedging*, one should either under-hedge or over-hedge. By providing a loss function that varies with the first two moments of the distribution of the hedging cost, the authors illustrated an ability of *reinforcement learning* to outperform regular *delta-hedging* with trading costs, and laid down interesting ideas for further developments, such as the introduction of other moments of the hedging cost distribution.

4.3 Results and discussion

Research design

This section will be devoted to studying the hedging strategy produced by the neural network for an At-The-Money *European Call option* with initial spot price $S_0 = 100$, using *discretized Black-*

S	K	vol	r	q	T (in days)	N (in days)
100	100	0.2	0.0	0.0	365	30

Table 1: Table 1: *Option parameters we will use for our computations.*

learning rate	epochs	batch size	hidden layers	neurons per layer	loss
0.005	10	500	2	25	<i>entropy</i>

Table 2: Table 2: *Algorithm parameters we will use for our computations.*

Scholes as a benchmark. A *simple neural network* with $L = 3$ and $L_i = \{1, 25, 25, 1\}$ shall be used in our research. The input data for the first two sets shall be taken from the *discretized* price dynamics of the underlying defined in (4.4).

Outcome and benchmark comparison

As expected, the algorithm is capable of correctly replicating the payoffs of the *European Call* option when evaluated under the previously introduced parameters. Minor changes are observed when we tweak them a little. For example, the prediction for the price gets more precise with a lower batch size and learning rate. However, the computation time that is required under those new conditions makes it a losing trade-off. An even larger decrease of those parameters combined with more *epochs* would cause *over-fitting* to appear, which happens when the algorithm is trained to decipher an exact relationship in the training data, making it unable to detect resembling relationships in new testing data. Here are the results for a given random set of underlying asset paths. Let us remark that the approximation is accurate, as the PnL obtained by using the algorithm is close to the real one computed using *Black-Scholes*, meaning that the δ parameters found by the network to replicate the price of the option are coherent.

We also notice that increasing the number of epochs to 50 does not significantly increase the quality of the prediction, although the PnL distribution is logically closer to what is obtained using the benchmark, per the graph below. Overall, the model appears to capture well the relationship between the asset moves and the price of the *European Call* option, when *entropy* is used as a loss function.

4.4 Introducing Heston stochastic volatility

Context and relevance of the research

Assuming constant volatility is one of the most substantial drawbacks encountered when working under *Black-Scholes*, as it reduces considerably the approximation for the hedging parameters of an

Black-Scholes price	Monte-Carlo price	Algorithm price
2.287	2.243	2.375

Table 3: Table 3: *Price results for a given simulation with 10 epochs.*

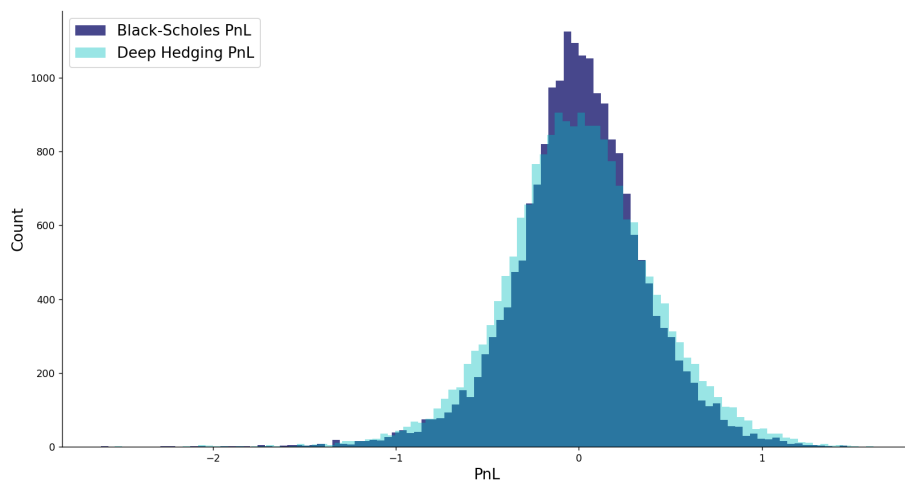


Figure 1: Figure 1: *Deep Hedging PnL against Black-Scholes benchmark with 10 epochs.*

Black-Scholes price	Monte-Carlo price	Algorithm price
2.287	2.313	2.358

Table 4: Table 4: *Price results for a given simulation with 50 epochs.*

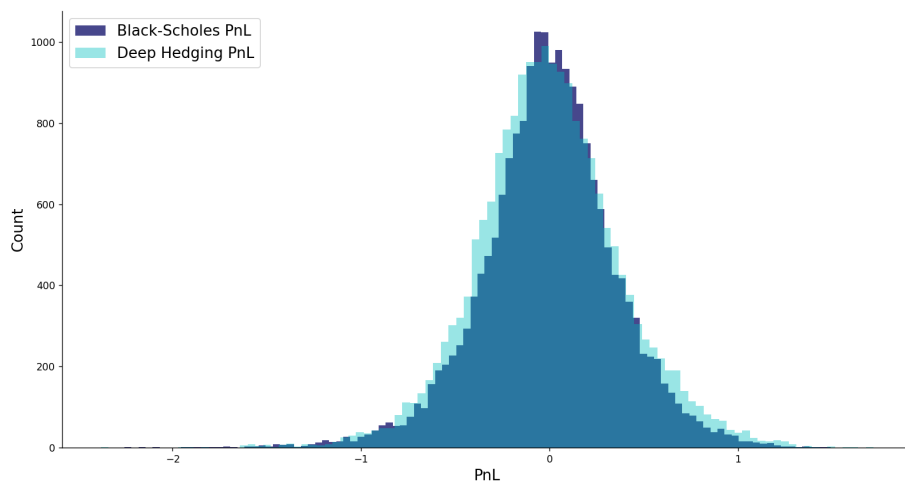


Figure 2: Figure 2: *Deep Hedging PnL against Black-Scholes benchmark with 50 epochs.*

v_0	κ	θ	ξ	ρ
0.0654	0.6067	0.0707	0.2928	-0.7571

Figure 3: Table 5: *Calibrated Heston parameters.*

Black-Scholes price	Monte-Carlo price	Algorithm price
2.287	3.089	3.194

Table 5: Table 6: *Price results for a given simulation with 10 epochs.*

option. Therefore, we would prefer to work under *Heston* dynamics, which considers the volatility of the asset as a stochastic process. We will illustrate how successful the artificial neural network is at retrieving the fundamental patterns in such new data. The architecture of the algorithm studied in the preceding section is to be used again, as we shall only change the input data, being derived from the log-transformed discretized price paths for the asset s and its volatility ρ , defined in (4.5) and (4.6).

Results and conclusions

To work with *Heston*, we needed to introduce calibrated parameters for the model. We decided to use those computed in [24]. Those parameters verify the *Feller condition*.

We expected the algorithm to continue to produce coherent *hedging parameters* compared to the *Black-Scholes* benchmark. For only 10 epochs however, the results were shifted upwards. This is probably due to the higher complexity of the relationship in the asset price dynamics caused by the introduction of a stochastic volatility.

It gets slightly better when increasing the number of epochs to 50, but the downward shift in PnL proposed by the algorithm seems to be persistent. However, we shall also envision that the benchmark may bear some responsibility for this gap. Indeed, we can see through the *Monte-Carlo* price, which is computed as the discounted average of all future payoffs, that it is a lot closer to what the algorithm produces. We can emit the hypothesis that because of the added uncertainty caused by the stochasticity of the volatility, the option gets more expensive. The algorithm may not entirely be wrong considering the latter.

All in all, the algorithm seemed to capture with a surprising accuracy the dynamics behind pricing and hedging an option relying on a single underlying asset, although some inconsistencies appeared when testing the network under *Heston* dynamics and few epochs. The final parts of this paper will focus on adapting and testing our algorithm in a multi-asset option context.

Black-Scholes price	Monte-Carlo price	Algorithm price
2.287	3.029	3.165

Table 6: Table 7: *Price results for a given simulation with 50 epochs.*

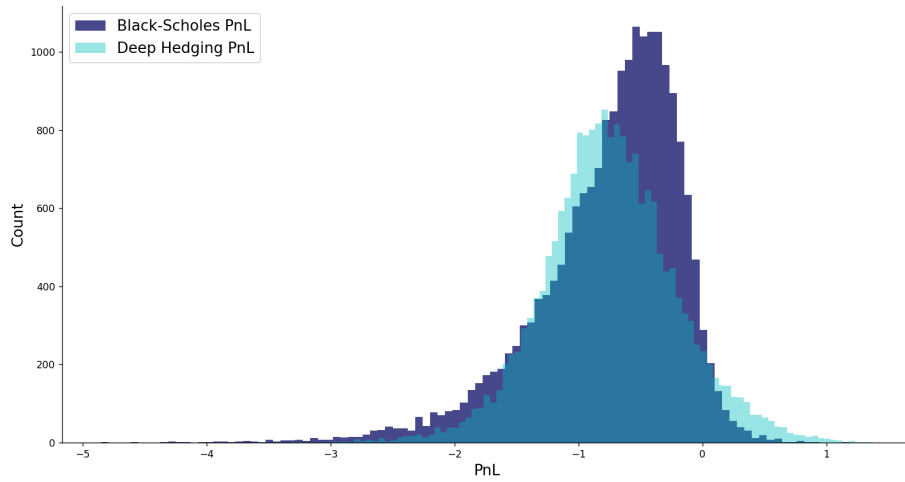


Figure 4: Figure 3: *Deep Hedging PnL against Black-Scholes benchmark with 10 epochs.*

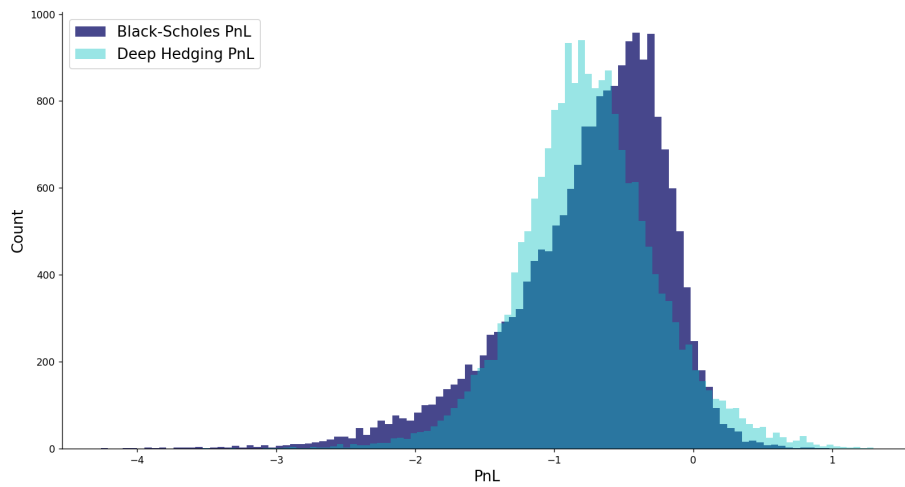


Figure 5: Figure 4: *Deep Hedging PnL against Black-Scholes benchmark with 50 epochs.*

5 Deep Hedging Rainbows

5.1 Financial Theory

Defining correlation options

One of the main challenges in portfolio management is the handling of risk exposure, to an asset class or a market sector for example. Although partly done through *hedging*, another fundamental strategy that is heavily used to reduce any risk exposure is known as *diversification*, which deals with how capital is allocated in the first place, in such a way as to minimize the risk of the portfolio.

The key idea behind *diversification* is that we consider the *correlation* between the movements of several asset prices. It is often perceived as preferable for the assets of a portfolio to be uncorrelated, as the plunge of one's price has lower chances of affecting the price of the other assets in our portfolio, hence offering protection. One can therefore see the potential of speculating on *correlation*, and several of the most traded derivatives on the market are purely based on such.

Rainbow options are correlation options. As was previously introduced, they are exotic derivatives relying on the performance of several underlying assets, each being a *color* of the rainbow. Several different types of payoff structures for the rainbow option can exist on the market, allowing for any investor with a specific view on the correlation of some assets to find an interest in trading the option. For example, a basket of two underlying stocks allowing the buyer to purchase the worst performing one can be perceived as an ideal protection, as long as the correlation between both assets is high, and is called a *worst-of call option*. The latter is the most popular of the class, and shall be studied for the rest of the section. The payoff Π of a *worst-of call option* on n underlying assets is given by the following equation, with S_i and K being the spot and strike prices of the underlying asset i at maturity T .

$$\Pi = \max \left(0, \min_{1 \leq i \leq n} (S_i(T)) - K \right) \quad (5.1)$$

As was already introduced in *Chapter 4*, multi-asset options are too complex for a closed-form *present value* to be easily computed, and analytical approximations using *Monte-Carlo* are accessible solutions for pricing and hedging purposes. The following sub-sections will lay out the research design for the use of artificial neural networks as a potentially efficient alternative method for such purposes.

Price and sensitivities of rainbows under Stulz

An analytical solution for the price of a *worst-of-two call option* was introduced by [25], along with an intuitive formula to compute its sensitivity to first-order price moves of its two underlying assets. We shall successively introduce those results. The latter will allow us to compute the two *delta-hedging* parameters according to the two spot prices at any moment. In its *training phase*, the neural network will be fed with a three-dimensional matrix filled with input data, which can be seen as being two-dimensional matrices for each simulation composed of the two stock price paths. Let us now lay out the theoretical foundations that led to the pricing and hedging formulas for European *rainbow* options.

The assumptions required are the same as those defined for *Black-Scholes* in the previous chapter, with the two assets following the stochastic differential system defined below. Let us notice that

those dynamics are different than the *Multi-asset geometric Brownian motion*. We will study this difference later.

$$\begin{cases} dS_t^i = \mu_i S_t^i dt + \sigma_i S_t^i dB_t^i & \text{with } i \in \{1, 2\} \\ dB_t^1 dB_t^2 = d\rho \end{cases}$$

We assume that ρ , μ_i and σ_i for $i \in \{1, 2\}$ are constants. Under the *no-arbitrage* condition, finding the value of the option comes down to computing the value of a portfolio P which replicates its payoffs. So, following *Ito's Lemma*, we derive the dynamics of P as a function of the spot prices, as well as the time to maturity.

$$\begin{aligned} dP(S_1, S_2, \tau) &= \frac{\partial P}{\partial S_1} dS_1 + \frac{\partial P}{\partial S_2} dS_2 - \frac{\partial P}{\partial \tau} dt \\ &+ \frac{1}{2} \left(\frac{\partial^2 P}{\partial S_1^2} S_1^2 \sigma_1^2 + \frac{\partial^2 P}{\partial S_2^2} S_2^2 \sigma_2^2 + 2 \frac{\partial^2 P}{\partial S_1 \partial S_2} S_1 S_2 \rho \sigma_1 \sigma_2 \right) dt \end{aligned}$$

Given that the above defined partial differential equation is verified, P is self-financing. By noting that when either one of the assets has price 0 the option is worthless, and using the constraint defined in (5.1), we can find the analytical solution to the price R of a *worst-of two call* option [25], with strike price K .

$$R = S_1 \mathcal{N}_2(\eta_1, \beta_1, \rho_1) + S_2 \mathcal{N}_2(\eta_2, \beta_2, \rho_2) - K e^{-r\tau} \mathcal{N}_2(\gamma_1, \gamma_2, \rho)$$

There, we have that $\mathcal{N}_2(\eta, \beta, \theta)$ is the bivariate cumulative standard normal distribution, η and β being the two upper limits of integration, and θ being the correlation coefficient. We also detail the simplifications that were made above.

$$\begin{aligned} \eta_i &= \frac{1}{\sigma_i \sqrt{\tau}} \left(\ln \left(\frac{S_i}{K} \right) + \left(r + \frac{\sigma_i^2}{2} \right) \tau \right) & \gamma_i &= \eta_i - \sigma_i \sqrt{\tau} \\ \sigma^2 &= \sigma_1^2 + \sigma_2^2 - 2\rho\sigma_1\sigma_2 & \rho_i &= \frac{\rho\sigma_j - \sigma_i}{\sigma} \end{aligned}$$

$$\beta_i = \frac{1}{\sigma \sqrt{\tau}} \left(\ln \left(\frac{S_j}{S_i} \right) - \frac{\sigma^2 \sqrt{\tau}}{2} \right)$$

Finally, one can compute the partial derivative of the price of the *rainbow* option with respect to the two assets, so as to define the *delta-hedging* parameters [25].

$$\begin{aligned} \delta_i = \frac{\partial R}{\partial S_i} &= \mathcal{N}_2(\eta_i, \beta_i, \rho_i) + \mathcal{N}_1 \left(\frac{\eta_i - \rho_i \beta_i}{\sqrt{1 - \rho_i^2}} \right) e^{-\frac{1}{2} \beta_i^2} \frac{1}{\sqrt{k}} \\ &- \left(\frac{S_j}{S_i} \right) \mathcal{N}_1 \left(\frac{\eta_j - \rho_j \beta_j}{\sqrt{1 - \rho_j^2}} \right) e^{-\frac{1}{2} \beta_j^2} \frac{1}{\sqrt{k}} \end{aligned}$$

With $j \in \{1, 2\}$, $j \neq i$ and $k = \min\{\ln(S_j)\}$. The design of our further research will be the following. The input data that will be fed into the algorithm will consist of the paths taken by the two assets. The algorithm will try to learn key features in the data, so that when introduced to new paths, the network is able to produce coherent and optimal hedging parameters. We will then compare those

results with our benchmark, to assess if the algorithm can be used as a substitute *rainbow* hedging method.

The computation of the cumulative bivariate normal probability $\mathcal{N}_2(\eta, \beta, \theta)$ is to be approximated. For the rest of this paper, we will consider the algorithm proposed by [11], whose surprisingly accurate method grants us four-decimal correct approximations. The detailed application can be found in the code.

Multi-asset Brownian motion extension

In the setting where the price dynamics of two assets are to be generated, one has to consider the correlation in their movements. Whereas we could be tempted to proceed as in *Chapter 4* while modelling *Heston* co-movements of the spot and the volatility, here we must remark that the influence is bilateral. To take such into account, we naturally choose to work with an extension of the *geometric Brownian motion* defined earlier for single asset dynamics. A *multidimensional* geometric Brownian motion can be specified through a system of stochastic differential equations, assuming S^i with $i = \{1, 2\}$ our assets.

$$dS_t^i = \mu_i S_t^i dt + \sigma_i S_t^i dB_t^i \quad (5.2)$$

Considering the *correlation* between those two stochastic processes, we define by \mathcal{M} the *covariance matrix* associated with the two Brownian motions.

$$\mathcal{M}_{ij} = \rho_{ij} \sigma_i \sigma_j$$

By recalling that a *Brownian motion* B with zero mean and said *covariance* can be written as AB , with A the *Cholesky* factor of \mathcal{M} , such that $AA^T = \mathcal{M}$, we can rewrite the system defined in (5.2) as the following.

$$dS_t^i = \mu_i S_t^i dt + \sum_{j=1}^2 A_{ij} S_t^i dB_t^j$$

Finally, and to allow for practical implementation, we decide to *discretize* such system. Let us define the following algorithm for simulating multidimensional *geometric Brownian motions* with the price log-transformed, such that $s_t = \ln(S_t)$.

$$s_t^i = s_{t-1}^i - \frac{\sigma^2 T}{2N} + \sqrt{\frac{T}{N}} \left(\sum_{j=1}^2 A_{ij} Z_k^j \right) \quad (5.3)$$

Those are the *discretized* price dynamics for the two underlying assets on which our exotic option is to be studied. We notice that in such context, the correlation coefficient ρ is constant, which remains unrealistic but makes computations easier. We recall that the price dynamics are evaluated under \mathbb{P} , so that $\mu_i = 0$ [2].

Multi-asset dynamics with jump-diffusion under Kou

The final and most exciting part of our research will be to evaluate the performance of our deep learning algorithm when fitted with stochastic paths for the two underlying assets endowed with random and unexpected large price moves. These sudden trends are characterized by *jumps*, and following the work of [20] on multivariate jump-diffusion models for asset pricing, we can derive the

following *stochastic differential equation* for two assets, and remark the similarity with the system defined in (5.2) for $i, j \in \{1, 2\}$, $i \neq j$.

$$dS_t^i = \mu_i S_t^i dt + \sum_{j=1}^2 A_{ij} S_t^i dB_t^j + d \left(\sum_{k=1}^{N(t)} (V_k^i - 1) \right) \quad (5.4)$$

We adopted the same notations as previously for the *Cholesky* matrix A . The final term between parentheses characterizes the additional jump part, described by a *Poisson* process $N(t)$, where jumps are denoted V_k . We consider two types of jumps, the first one being an individual jump that affects only one of the two assets, and is defined with the *Poisson* rate λ_i for $i \in \{1, 2\}$. The second being a common jump that affects both our assets, with λ_c being the corresponding *Poisson* rate. The final rate λ of our *Poisson* process is therefore $\lambda = \lambda_c + \lambda_1 + \lambda_2$. This illustrates how complex it would be to consider more than two underlyings.

The jump V_k is such that its log-transform has the following distribution, with \mathcal{M} the covariance matrix, μ_c the vector for the means of the two assets, and μ_i and σ_i respectively the mean return and volatility of asset i . Let us remark that our *individual* and *common* jumps follow respectively one-dimensional and two-dimensional *asymmetric Laplace distributions* that we will denote \mathcal{AL} [20].

$$(\ln(V_k^1), \ln(V_k^2)) = \begin{cases} \mathcal{AL}_2(\mu_c, \mathcal{M}) & \rightarrow \text{probability} = \frac{\lambda_c}{\lambda} \\ (\mathcal{AL}_1(\mu_1, \sigma_1^2), 0)' & \rightarrow \text{probability} = \frac{\lambda_1}{\lambda} \\ (0, \mathcal{AL}_1(\mu_2, \sigma_2^2))' & \rightarrow \text{probability} = \frac{\lambda_2}{\lambda} \end{cases}$$

Computation is made easier using the following relationship, where μ_i is the mean vector of the assets, \mathcal{M}_i is the covariance matrix, \mathcal{Z} is an exponential law and i is the number of assets [19]. We remark that for *individual* jumps, \mathcal{AL}_1 is a scalar, and when *common* jumps are considered, \mathcal{AL}_2 is a two-entry array.

$$\mathcal{AL}_i(\mu_i, \mathcal{M}_i) = \mu_i \mathcal{Z} + \sqrt{\mathcal{Z}} \mathcal{N}_i(0, \mathcal{M}_i)$$

From then on, we can derive the discrete dynamics of the two asset paths, considering Z_k^i a cumulative standard normal distribution and N a *Poisson* process with rate λ . All three are assumed to be independent of the jumps themselves.

$$s_t^i = s_{t-1}^i - \frac{\sigma^2 T}{2 N} + \sqrt{\frac{T}{N}} \left(\sum_{j=1}^2 A_{ij} Z_k^j \right) + \sqrt{N \left(\lambda \frac{T}{N} \right)} \Lambda_i \quad (5.5)$$

We chose to denote by Λ_i the distribution for the log-transform of the jump, which could be either individual or common to both assets. Let us remark that if the jump is individual to i , then $\Lambda_j = 0$. Λ is a two entry vector that impacts both assets at every period, based on the probability distribution defined above.

The *Python* implementation will then be straightforward. We will build a module that is capable of producing the joint dynamics of our two assets over N time steps, and we will then loop for a given number of simulations to produce the *training set* that is to be given as inputs for the algorithm.

Stulz price	Monte-Carlo price	Algorithm price
2.393	2.580	8.304

Table 7: Table 8: *Price results for a given simulation with 10 epochs.*

5.2 An extensive literature review

The few and recent papers that tackled the use of artificial neural networks in pricing and hedging problems for exotics options have illustrated the potential of the method in such a context. In his study of *Bermudian* options, [22] demonstrated an interesting technique to semi-statically hedge high-dimensional and path-dependant claims, by defining an upper and lower bound for the price of the option. Beyond illustrating the simplicity and efficiency of the model for both pricing and hedging purposes, the neural networks used are flexible, as they have been tested for several types of options with linear and nonlinear payoff structures, whose outcome was demonstrated to be at least as good as the benchmark, using *mean squared error* (2.7) as a loss function.

Some other developments regarding *rainbow options* were seen with [5], where the author demonstrated that the algorithm could not produce satisfying *present values* for such options, although it was able to price an option as a *Monte-Carlo* method would. The reason is that the network was not able to correctly decipher the pricing function for the option, contrarily to what was demonstrated by [16]. The reason advanced by [5] was the lack of a qualitative data set to be fed to the algorithm, an issue that was further studied in [12], where the author successfully managed to value basket options on six underlyings, with prodigious pace when compared to *Monte-Carlo* simulations.

5.3 Results and discussion

Brief overview of the research design

In this section, we will tackle the problem of producing coherent hedging parameters for a *worst-of call option* on two underlying assets with same initial spot price $S_0^i = 100$, and whose dynamics are defined in (5.2). As a benchmark, we shall use the analytical formula defined above for *delta* computation of said rainbow option. The same architecture as in the preceding chapter shall be used. The loss function chosen is the *entropy risk measure* (2.6). The input data that we load into the deep learning algorithm will be comprised of stochastic paths for the two assets as defined in (5.2). The final data used to verify the performance of the algorithm will also be generated randomly.

Outcome and benchmark comparison

Given the complexity of that new algorithm, we did not initially expect very accurate results on the first try. Indeed, hedging an option relying on two underlying assets required the network to account for a two-dimensional set of inputs, as well as being able to produce two outputs. Keeping the same parameters as those introduced previously, we can observe that the outcome of the algorithm is not entirely off the chart, although major refinements will need to be implemented. In that first try with regular spot dynamics, let us observe that the algorithm was able to produce a good overall replication of the *worst-of-two call* option, with the *profits and losses* matching quite well the benchmark from *Stulz*.

Let us notice that contrary to the previously studied algorithm for vanilla hedging, the dispersion of the *profits and losses* is much higher when hedging rainbow options. The algorithm and the

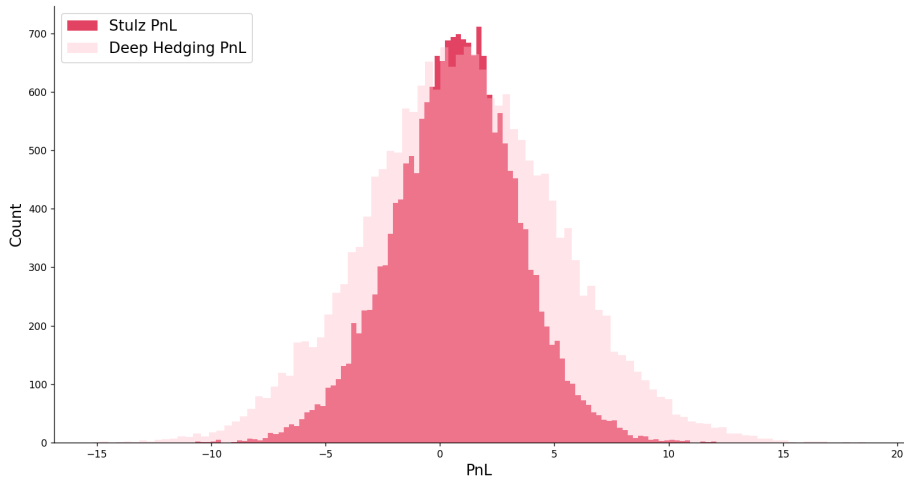


Figure 6: Figure 5: *Deep Hedging PnL against Stulz benchmark with 10 epochs.*

Stulz price	Monte-Carlo price	Algorithm price
2.393	2.507	3.541

Table 8: Table 9: *Price results for a given simulation with mse as a loss function.*

benchmark are a lot less precise in the production of a hedging strategy against the moves of the two assets for which the option is written on, which makes sense given the added complexity embedded with both the dynamics and the payoff structure of the derivative.

The increase in the number of *epochs* did not strongly increased the quality of the outcome, and it was observed that the model purely stopped learning after having passed the threshold of 20 *epochs*, while increasing the *learning rate* to 0.01 to accelerate the convergence towards *Stulz* benchmark.

Using the *mean squared error* (2.8) this time radically improves the quality of our results, and the price given by the algorithm now seems to converge towards the *Stulz* benchmark, using once again the model parameters defined in *Table 2*.

5.4 Multivariate case jump-diffusion extension

Context and relevance of the research

While it makes sense for our deep learning algorithm to be tested for hedging purposes under regular market dynamics, it comes as even more interesting to verify its robustness under large and unexpected moves in the underlying asset prices. Indeed, it is during those rare and unpredictable events that the hedging parameters produced are more likely to be off the chart, forcing traders to

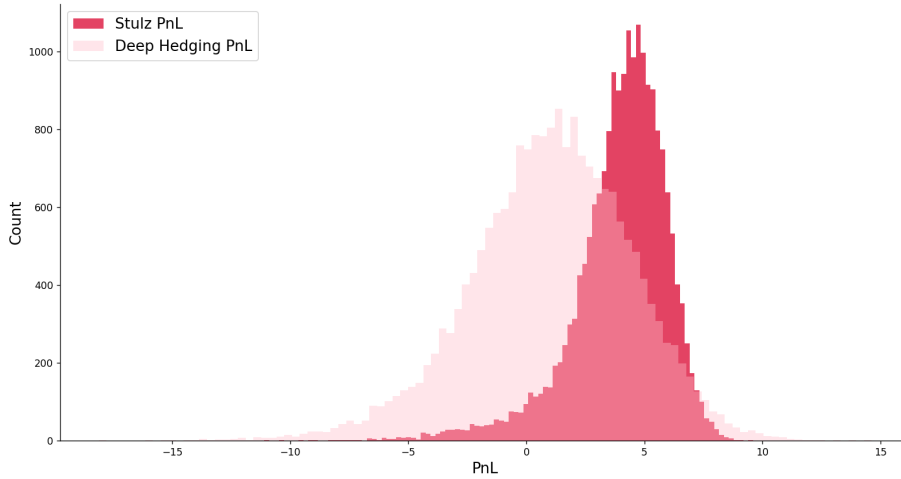


Figure 7: Figure 6: *Deep Hedging PnL against Stulz with mse as a loss function.*

learning rate	epochs	batch size	hidden layers	neurons per layer	loss
0.01	10	200	4	25	<i>mse</i>

Table 9: Table 10: *Algorithm parameters we will use for our computations.*

manually re-calibrate their strategies. This sub-section will be devoted to running our algorithm in such a context, by providing the artificial neural networks with asset paths generated using the method defined above [20], with the dynamics introduced in (5.5). The benchmark remains the *discrete delta-hedge* [25].

Results and conclusions

The presence of jumps in the dynamics of an underlying asset is usually extremely difficult to consider for standard valuation models, so our expectations regarding the accuracy of our algorithm are limited for this first try. Adding to that the duality of assets to be considered, and we obtain joint dynamics that can be extremely tricky to analyze, even with sophisticated neural networks.

That being said, the large number of experiments we ran provided prices that were far from incoherent, although still wrong. The model initially could not perceive the relationship stemming from those new dynamics, and the resulting *parameters* and *prices* were extremely far from our benchmark. Tweaking the parameters then allowed us to refine our model and obtain cleaner outputs. We chose to increase the number of *hidden layers*, and we also used a larger *learning rate* and a smaller *batch size*. The *mean squared error* (2.8) was eventually the preferred loss function, as it was shown to provide stronger results than the *entropy* did in the preceding section. We will however show that the dispersion in the *profits and losses* remains extremely large, which massively jeopardizes the overall quality of the replication, and thus of the *delta-hedging* strategy.

Stulz price	Monte-Carlo price	Algorithm price
2.393	1.397	14.081

Table 10: Table 11: *Price results for rainbow options with jump diffusion dynamics.*

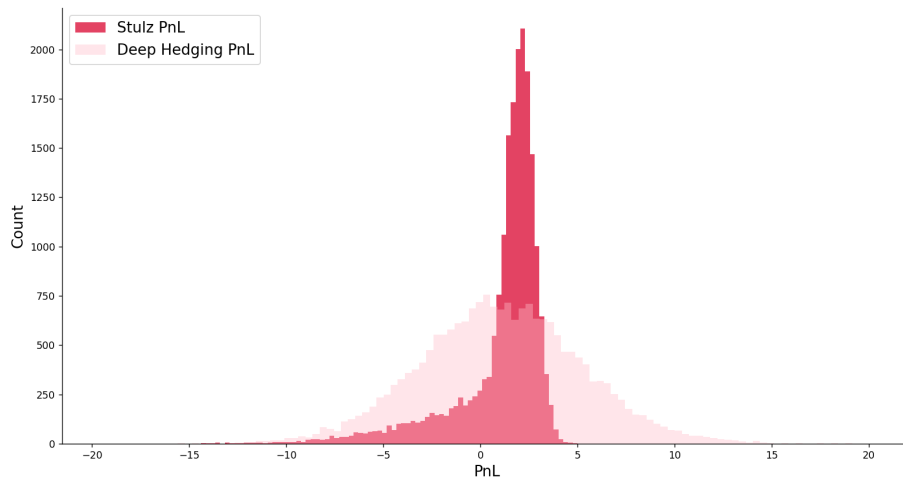


Figure 8: Figure 7: *Deep Hedging PnL against Stulz with jump diffusion dynamics.*

As one can observe with the results above, the algorithm was not capable of approximating the correct *hedging* parameters for the rainbow options under such dynamics, and nothing changes with an increased number of *hidden* layers or an increased *learning rate*: the algorithm seems to always converge towards a price that is too far from what it should connect with.

6 Conclusion and discussion

6.1 Research outcome

In this thesis, we aimed at using the advantageous architecture of neural networks to design an algorithm capable of hedging financial derivatives. We first demonstrated the remarkable ability of the network to decipher simple single-asset dynamics and hedge a *European Call* option, although a better *Heston* calibration and an improved benchmark might have shown stronger results.

We then tried to adapt our algorithm to a multi-asset situation by considering a *worst-of two Call* option, for which the results were less satisfying. The algorithm was not capable of precisely capturing the hedging dynamics behind the exotic option, and many factors can be coined as responsible for such, starting with the intertwined dynamics of the two underlying assets, for which the algorithm struggled to extract a relationship that would have given the exact *delta-hedging* parameters. Increasing the number of *epochs* and the *learning rate* did not significantly increase the quality of the outcome.

Then finally, when adding another layer of complexity with a *jump diffusion* parameter for both asset dynamics, we were able to observe some limits to the deep learning method, as it was clear that the model was not able to correctly decipher the embedded functions and relationships in that data, and so for a large choice of model parameters. Some improvements could probably be foreseen with the use of *recurrent* neural networks instead, which would allow a deeper perception of those complex dynamics.

6.2 Limits of the deep learning method

This study was concentrated on studying vanilla and fairly restricted exotic options, as we believe that despite the remarkable computational power of artificial networks, they would most likely fail to capture more complex relationships, considering for example a *worst-of ten Call option*, which would require the manipulation and approximation of extremely intertwined dynamics. Dealing with such issues may be realized through a larger *training* set and an increased variety in the generated price dynamics, considering for example a stochastic correlation matrix between the underlyings. But then again, managing to hedge single exotic derivatives fails to help the trader who wishes to hedge an entire portfolio.

The final and most inherent shortcoming to working with artificial neural networks is the *black-box* problem. As introduced earlier, those algorithms approximate non-linear relationships in the input data during the *training* phase [16], and then use such functions on new data during the *testing* phase. Those functions remain invisible to the user, so one might find it difficult to entirely trust the outcome of the network, especially in the context of hedging derivatives, where the stakes can be very high. The deep learning model can then at best be used jointly with another more classic and reliable method, which will at least reduce the degree to which traders have to rely on their intuition to re-calibrate their strategies. The algorithm could also offer clues for innovative and potentially efficient new strategies, reinforcing its position as a research tool for traders.

6.3 Further research

Reflecting on this research, several improvements could be foreseen in the context of *hedging rainbow* options, particularly through three major refinements: the necessity to consider *stochastic correlations* between the colors of the rainbow, and the possibility to implement *trading signals* in the form of *forecasts* for the *volatility* and the *correlation* matrices of the underlyings.

Considering simple correlation trading signals

The high degree of complexity that implementing those methods in such context would require refrained us from wanting to do so, but the need to further train the algorithm in a context that aspires to imitate real market dynamics will inevitably lead us to such future developments. We could however consider a direct correlation *trading signal* that would encompass the first two moments of the distribution for the correlation between our two assets. Using such might let the algorithm observe the appearance of specific patterns before episodes of correlation moves and understand their consequences on the hedging parameters, in order to adjust the strategy consequently.

Volatility forecasts through quantile regression

Following the work of [27], we propose to implement quantile regression to determine volatility forecasts for the returns of our underlyings, and use those as trading signals, introduced as additional inputs to our deep learning algorithm. This method relies on the analysis of stock return autocorrelation on several sub-parts of the overall distribution, based on which we can infer a general autocorrelation pattern which we will use to determine future volatility levels.

This method was proven robust, for it does not assume a fixed conditional distribution of stock returns, an assumption that truly harmed other simpler models. Indeed, it was shown by [27] that autocorrelation on both extremes of the distribution is different. When stock prices are increasing, their future returns appeared as negatively correlated with their past returns, which is also true contrariwise. Using such might allow the algorithm to refine its hedging strategy, by considering deeper dynamics than those observable with current models.

Covariance forecasts with support vector regression

In a market where the intertwined moves of hundreds of assets need to be considered, having an accurate forecast for the complete *covariance* matrix of the returns is of much more help for our analysis, as the sole consideration of volatility forecasts omits the pondering of *correlation* coefficients between the assets.

As advanced by [13], an innovative, stable and flexible method can be observed in *support vector regression* to produce forecasts for covariance matrices, for which the major advantage is the surprising reliability of the method in highly tumultuous markets, when accurate forecasts are the most needed. Another significant development is the growing efficiency of the method when compared to univariate generalized autoregressive conditional heteroskedasticity models [13].

The complete methodology introduced by [13] is decomposed into five steps, during which we shall successively extract the *Cholesky* from the *range-based* covariance matrix of returns that is to be first estimated, and then forecast the individual *Cholesky* factors instead of the whole matrix, for this decomposition allows the positive definiteness of the forecasted covariance matrix. We

then produce our covariance forecast by applying the reverse decomposition, using the previously estimated *Cholesky* factors.

The efficiency of *support vector regression* mainly comes from its ability to consider nonlinear data-generating processes, whereas other methods assume their linearity. This is crucial, as the nonlinearity of the dynamics of assets was observed in several studies [13]. Exploring the use of such methods for an increasingly accurate representation of the market dynamics, in the context of training a neural network to hedge financial derivatives, remains the most exciting further development that is to be realized following this paper.

Bibliography

- [1] An Yunbi, Suo Wulin (2003), *The performance of option pricing models on hedging exotic options*, Working Paper, Queen's University.
- [2] Back Kerry (2005), *A course in Derivatives Securities: Introduction to Theory and Computation*, Springer Finance Textbook, 372 pages.
- [3] Black Fisher, Scholes Myron (1973), *The pricing of options and corporate liabilities*, Working Paper, The University of Chicago Press, The Journal of Political Economy, Vol. 81, No. 3 (May - Jun., 1973), pp. 637-654.
- [4] Boyle Phelim (1977), *Options: A Monte Carlo approach*, Working Paper, Journal of Financial Economics, Volume 4, Issue 3, May 1977, pp. 323-338.
- [5] Brostrom Axel, Kristiansson Richard (2018), *Exotic derivatives and deep learning*, Master's Thesis, KTH Royal Institute of Technology.
- [6] Buehler Hans, Gonon Lukas, Teichmann Josef, Wood Ben (2018), *Deep hedging*, Working Paper, JP Morgan, ETH Zürich.
- [7] Cao Jay, Chen Jacky, Hull John, Poulos Zissis (2020), *Deep hedging of derivatives using reinforcement learning*, Working Paper, Journal of Financial Data Science, 3, pp. 10-27.
- [8] Carr Peter, Madan Dilip (1998), *Option valuation using the Fast Fourier Transform*, Journal of Computational Finance 2, pp . 61-73.
- [9] Carverhill Andrew, Cheuk Terry (2003), *Alternative Neural Network Approach for Option Pricing and Hedging*, Working Paper, The University of Hong Kong.
- [10] Chollet François (2021), *Deep learning with Python*, Manning, 384 pages.
- [11] Drezner Zvi (1978), *Computation of the bivariate normal integral*, Mathematics of Computation, 32 (January 1978), pp. 277-279.
- [12] Ferguson Ryan, Green Andrew (2018), *Deeply learning derivatives*, Working Paper, Version 2.1, Scotiabank.
- [13] Fiszeder Piotr, Orzeszko Witold (2021), *Covariance matrix forecasting using support vector regression*, Working Paper, Nicolaus Copernicus University in Torun, Applied Intelligence, pp. 7029-7042.
- [14] He Kaiming, Zhang Xiangyu, Ren Shaoqing, Sun Jian (2015), *Delving Deep into Rectifiers: Surpassing Human-Level Performance on ImageNet Classification*, Working Paper, Microsoft Research.
- [15] Heston Steven (1993), *A closed-form solution for options with stochastic volatility with applications to bond and currency options*, The Review of Financial Studies. 6 (2), pp. 327-343.

- [16] Hornik Kurt (1991), *Approximation capabilities of multilayer feedforward networks*, Working Paper, Neural Networks 4, no. 2, pp. 251-257.
- [17] Hutchinson James, Lo Andrew, Poggio Tomaso (1994), *A nonparametric approach to pricing and hedging derivative securities via learning networks*, Working Paper, The Journal of Finance Vol. 49 No. 3, Massachusetts Institute of Technology.
- [18] Kingma Diederik, Lei Ba Jimmy (2015), *Adam: a method for stochastic optimization*, Conference paper, OpenAI, University of Toronto.
- [19] Kotz Samuel, Kozubowski Tomasz, Podgorski Krzysztof (2003), *The Laplace distribution and generalizations*, Textbook, Boston, MA, pp. 239-272.
- [20] Kou Steven (2008), *Jump-diffusion models for asset pricing in financial engineering*, Survey article, J.R. Birge and V. Linetsky, Handbooks in OR and MS, Vol. 15, pp. 73-116.
- [21] Kozira Michal (2018), *Deep learning approach to hedging*, Candidate Number: 1023650, Master's Thesis, Oxford University.
- [22] Lokeshwar Vikranth, Bhardwaj Vikram, Jain Shashi (2019), *Neural network for pricing and universal static hedging of contingent claims*, Working Paper, Cornell.
- [23] Ruder Sebastian (2019), *An overview of gradient descent optimization algorithms*, Working Paper, Insight Center for Data Analytics, NUI Galway.
- [24] Schoutens Wim, Simons Erwin, Tistaert Jurgen (2003), *A Perfect Calibration ! Now What ?*, Working Paper, University of Leuven.
- [25] Stulz René (1982), *Options on the minimum or the maximum of two risky assets: Analysis and Applications*, Working Paper, Journal of Financial Economics, University of Rochester, pp. 161-185.
- [26] Ye Ziqun (2013), *The Black-Scholes and Heston models for option pricing*, Master's Thesis, University of Waterloo.
- [27] Zhao Yixiu (2020), *Stock returns, quantile autocorrelation and volatility forecasting*, Working Paper, International Review of Financial Analysis.